Optimization of Energy Conservation and Energy Conversion of Super Hydrophobic Surfaces

[1]Gautam Kunal, [2]Prof. Sachin Jain, [3]Dr. Piyush Jain

M. Tech. Scholar, Department of Mechanical Engineering, Bansal Institute of Science and Technology, Bhopal (M.P.)[1]

Assistant Professor, Department of Mechanical Engineering, Bansal Institute of Science and Technology, Bhopal (M.P.)[2]

Head of Dept., Department of Mechanical Engineering, Bansal Institute of Science and Technology, Bhopal (M.P.)[3]

Abstract— The self-cleaning surfaces are of interest in various applications, e.g., self-cleaning windows, windshields, exterior paints for buildings, navigation-ships and utensils, roof tiles, textiles, solar panels and reduction of drag in fluid flow, e. g. in micro/nano-channels. Also, super hydrophobic surface can be used for energy conservation and energy conversion. When two hydrophilic surfaces come into contact, condensation of water vapour from environment forms meniscus bridges at asperity contacts which lead to an intrinsic attractive force. This may lead to high adhesion. Therefore, super hydrophobic surfaces are desirable. The hydrophobic interaction is mostly an entropic effect originating from the disruption of highly dynamic hydrogen bonds between molecules of liquid water by the non-polar solute. In this paper, method has been developed and applied to produce superhydrophobic surfaces by using low surface energy materials/coatings on hierarchical structure of surface with micro and nano scale roughness. Using the above method, 4 numbers each of hierarchically structured and fluorinated/ chlorinated SS430 specimen were prepared.

Keywords- Micro/Nano Channel, Surfaces, Energy Conservation, Energy Conversion

I. INTRODUCTION

Not alone the plants, the superhydrophobic research has been extended to animals, insects and marine life as well, where a variety of microstructural features have been revealed and correlated to the observed wetting characteristics, including superhydrophobicity. The wetting related research on insects, spiders, lizards and frogs, other aquatic animals such as fish, sharks and birds, as reviewed in has revealed and confirmed the role of microstructure on the superhydrophobicity and related functionalities. Certain other interesting functionalities such as colour iridescences on butterfly wings or superhydrophilicity and superoleophobicity on fish scale, anti-fogging property on a moth eye and many others are described in Specifically, the nano /micro-structured superhydrophobic surfaces on butterfly wings, mosquito eyes, water strider legs and bird feathers, have shown striking resemblances to superhydrophobic surface structures of plant life.

Butterfly Wings with multi-scale structures (Fig.1 a-c) are superhydrophobic and exhibit directional adhesion owing to an oriented one-dimensional arrangement with periodic overlapping micro-squamas covered by lamella-stacking nano-stripes as may be seen in the figure. Due to anisotropy in wing structure, the water can easily roll along the radial outward direction, but is tightly pinned in the opposite direction. Besides the superhydrophobicity, butterfly wings also exhibit structural color and directionally controlled fluorescence emission functionalities.

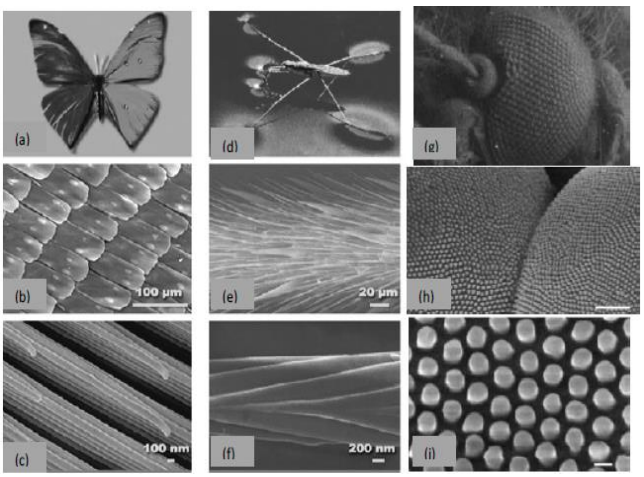

Fig1.11: Superhydrophobic surfaces in insects (a)Butterfly (b) SEM image of microstructure of butterfly wing (c) Magnified image in (b). [Acknowledgement Gao et al. [74](d) Pond skater (G.remigis) walking on water (e) SEM images of a pond skater leg showing numerous oriented microscale setae and (f) nanoscale grooved structures on a seta [Acknowledgement Gao and Jiang [75]](g) A Mosquito eye comprised of hexagonal close packing micro hemisphere (10µm) of (ommatidia) (h) two neighboring ommatidia (i) nanonipples covering an ommatida surface

Pond skaters (Gerris remigis), also referred as water striders (Fig. 1 d-f) are insects that live on the surfaces of ponds, slow streams and quiet waters. A pond skater has the ability to stand and walk upon a water surface without getting wet. It showed that the special hierarchical structure of the pond skater's legs, which are covered by large numbers of oriented tiny hairs (micro setae) (Fig.1 e) with fine nano-grooves (Fig. 1 f) and covered with cuticle wax, makes the leg surfaces superhydrophobic and is responsible

for the water resistance and enables them to stand and walk quickly on the water surface.

Mosquito eyes exhibit superhydrophobic antifogging properties to provide excellent vision. An SEM micrograph of a single eye is shown in (Fig. 1 g). It is composed of hundreds of microscale microspheres called ommatidia, (Fig. 1 h) which act as individual sensory units. These ommatidia are 26 micrometer in diameter and organize in a hexagonal closed packed (HCP) arrangement. At increased magnification, the surface of each micro- spherical ommatida is covered with nanoscale nipples (Fig. 1 i).It is observed that the nipples have an average diameter of 100 nm with a pitch of 47 nm and organized in a non- close-packed (NCP) array. It is the hierarchical structure (micro scommatida/nano nipples), that is responsible for superhydrophobicity. Many insects, birds, animals have shown similarity to hierarchal structure noticed on plant surfaces. Some of the representative cases are shown in Fig. 2. The microstructures of Beatles Walker (Homoptera Meimuna opalifera) and the Thunberg (Orthoptera Acrida cinerea cinerea) shown in Fig. 2 (b) and (c), respectively clearly show Hierarchal homogeneous protrusions with smaller dimensioned top structure, similar to lotus leaf. Similarly, the pigeon feather structure in Fig1.12c shows anisotropic structures similar to rice leaf. Many bird feathers exhibit hydrophobicity, besides providing for aerodynamic lift during flying, provide coloration for appearance as well as camouflage and provide an insulating layer to keep the body warm. As referred above, SEM image of the pigeon feather (pennae) is shown in Fig.1.12c. The morphology consists of a network formed by barbs and barbules made of keratin protein. It is this hierarchal morphology of barbs and barbules that plays an important role in hydrophobicity.

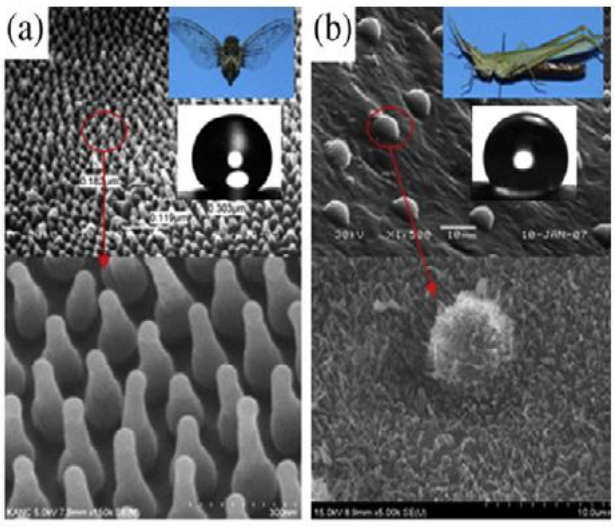

Fig. 2: Superhydrophobicity in insects and birds with similarities of microstructure to plant surfaces (a)-(b); the hierarchical homogeneous protrusions with smaller dimensioned top structure similar to lotus leaf

II. METHODOLOGY

On reviewing the literature, it is observed that the topic of superhydrophobic stainless steel surfaces, so far, has not been studied adequately for its various aspects. For instance, there are no studies for chemically roughened stainless that reveal the influence of etching parameters on the desired roughness structures. Also, there has not been enough data for creating desirable scales for hierarchical nano/microscale roughness on stainless steel for superhydrophobicity. Similarly, the issue of poor adhesion of structures, that are essentially required for obtaining the superhydrophobicity, has been mostly overlooked or not revealed. There is enough scope to research on some of these issues and the present thesis aims to fill these gaps. Accordingly, the choice of methods and methodology of this thesis is guided by investigating on above aspects and yet developing by simple inexpensive scalable methods for obtaining superhydrophobic steel surfaces.

The review of methods available in literature for preparing superhydrophobic metal surfaces presents various options, as made apparent in this chapter. The relevant options for the objects namely the facile, scalable, simple and inexpensive methods for this thesis however restrict the choice. Based on these objectives, following choice has been made for the protocol and methodology adopted in this thesis. The shortlisted methods that may meet the object in this thesis with their merits and demerits are presented in Table 1.

Table 1: Summarized View of Methods for Superhydrophobic Metals Including Steel

Surface structuring Technique (for Metals)	Merits	Demerits
Laser Ablation	Accurate controllable micro structures	Expensive Slow serial process Not suitable for Large are fabrication
Chemical Etch	Fast, facile inexpensive	Less control Acid use may require careful handling
Sol-gel Deposition	Purity Inexpensive Flexibility and simplicity	In stability of sol may lead to process inconsistency Long Sol preparation time (up tp 24hours or more) Poor Adhesion of deposited films (particularly Stainless steel)
Colloidal self-assembly	Fast Facile Can be made inexpensive Flexibility	May require suitable choice of colloidal particles Agglomeration of particles

From the shortlisted methods in the Table6.1 the following strategy and methodology for experiments and investigations has been adopted for the stainless steel, as also shown schematically in Fig 3:

(1) The stainless steel of commercial grades will be used for investigations.

(2) The steel specimen will be chemically etched using common acids, to get micro scale roughness.
(3) Over these micro roughened steel surfaces, nano scale roughness will be created by depositing silica nano particles by colloidal –assembly method.
(4) The silica nano particles for use of (3) will be derived by sol-gel synthesis of at least two nano dimensions in range of 50-200nm.
(5) The silica micro structured surface of steel will be treated by fluoro compound by solution methods. (6) The optimization of micro roughness in etched specimen in (2) will be carried out by measuring water contact angle.
(6) Similarly, the optimization of fluorinated silica layer deposition will be carried out by measuring contact angle. Here, hysteresis will also be measured.
(7) Stability of the prepared films in respect to UV stability temperature and pH will be determined.

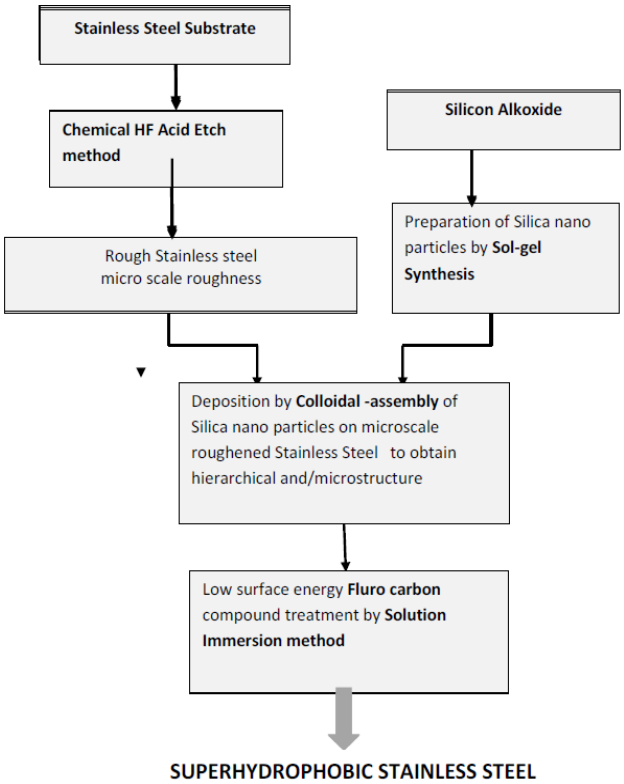

Fig 3: Methodology and Methods used in this thesis for investigations and development of Superhydrophobic Stainless steel.

III. EXPERIMENTS AND INVESTIGATIONS

As outlined in the work plan, we split the experiments in three tasks as following and show more explicitly in as Task-1. We experiment for Tasks 1 related to roughening of stainless steel by chemical etch.

Task-1: Preparation of Structured Stainless Steel by Chemical Etch

Materials: The steel substrate used for microstructuring is commercial grade Stainless Steel (SS) of grade SS 430 of composition typical and as specified by the vendor:

Composition of Stainless Steel grade 430

Analysis%	C	Mn	P	S	Si	Cr	Others	Fe
Typical	0.05	0.7	0.021	0.024	0.6	16-18	-	Rest
Vendor specified	0.12	1.0	0.04	0.03	1.0	16-18	0.75	Rest

For creating roughness, the HF acid (Reagent grade Fisher Scientific, 48−51%)) is used as etchant. For the post etch passivation, the HNO3 acid (Fisher Scientific, ACS grade, 68−70%)) is used. For low surface energy treatment, the fluoro carbon compound trichloro(1H,1H,2H,2H-perfluorooctyl) silane (PFOS) (purchased from Sigma-Aldrich, USA) has been used as hydrophobicity agent. Ultrapure de-ionized (DI) water (18.2M_cm-1) is used, obtained from Milli-Q water system.

IV. PREPARATION METHODS

Pre-etch Preparation The coupons of approx 1x1 cm are cut from the as received SS430 steel sheets. The SS coupons were degreased with an organic soap and cleaned ultrasonically. For the cleaning purpose, samples were first kept into soap solution for around 1 hour. The samples then rinsed with DI water and kept in a beaker which contained acetone for a period of 2 hours in an ultrasonicator. The obtained samples were further cleaned with DI water (Milli-Q) and dried using air. The surface of commercial SS is usually highly inert and not easily amenable for chemical reaction. For subsequent etching operation, the SS coupon surfaces were lightly ground to overcome the inertness and activate their surfaces.

The grinding was done manually using silicon carbide (SiC) emery paper successively in steps using gage 120, 400 800. The ground coupon becoming slightly hydrophobic (WCA~ 95o) compared to as received has been considered adequate as a test of removal of the contaminants and inert surface of the SS coupons. The ground SS coupons were degreased by organic soap and cleaned ultrasonically with de-ionized water and acetone. For subsequent etching operations, freshly ground and cleaned specimen were used within 2-days of aging. It has been observed during the course of experiments that longer duration aging can enhance the contact angle and thus influence the etching step. To minimize any such influences the specimen were etched within two days after being prepared by grinding and cleaning.

Chemical Etching Initial Etch experiments: The ground and cleaned SS coupons were etched in HF diluted with DI water in ratio of 1:5 by volume for various durations from 2min to 30 min (2,6,12,15,20,30min) at temperatures between 30-50o. The etched specimens were rinsed in copious amount DI water 2-3 times immediately after removal from the HF acid etch bath. To avoid and minimize re-oxidation of etched surface the specimen were passivated by immersing in diluted HNO3 (1:2 of water by volume) for a duration of about 10min. The passivated surfaces were ultrasonically cleaned using DI water for durations 5-10 min

to remove any remaining debris or contaminants arising from preceding steps and dried with flowing nitrogen. The dried samples were further kept in the oven at 120oC under vacuum for 2 hours for the removal of additional moisture from the surface of the samples and stored in evacuated dessicator for subsequent characterization of their roughness and morphology. All HF etched specimens were essentially passivated, hence now onwards any references for etched specimen denote for HF etched + passivated specimen, unless stated otherwise.

Modified etch experiments: The above etch procedure was adopted for the initial experiments. Based on these results more optimized parameters were used that are explained while discussing the results of the initial experiments in next section.

Deposition of Low surface energy material: To reduce the surface energy of the etched surface, the hydrophobicity agent fluoro carbon compound trichloro (1H,1H,2H,2H-perfluorooctyl) silane (PFOS) has been used. A diluted solution of PFOS 1-2 wt% in ethanol has been used. For coating PFOS on etched surfaces, the method of immersion/dip coating the etched specimen has been used. PFOS solution was prepared using magnetic- stirrer with the help of a magnetic-spin bar. The mixed fluoro solution was kept in capped bottles and vigorously stirred for 24 hours at room temperature. The etched specimens, as prepared above were immersed for duration of 1hour and after withdrawing from solution, were dried in oven at 70-80oC. For adequate coverage of rough surface, the immersion dipping procedure was repeated for 2-3 cycles.

Characterization of Roughness The micro/nanoscale roughness can be determined most conveniently by Optical Profilometery or by Atomic Force Microscopy (AFM). The AFM however should be used for relatively smoother surfaces where nanoscale roughnesses are expected. The Scanning electron microscopy with energy dispersive spectroscopy (SEM/EDX) can also be used though it is most useful for the information on morphology and for chemical nature of surface. In the present work, for determining roughness we have used optical profilometer.

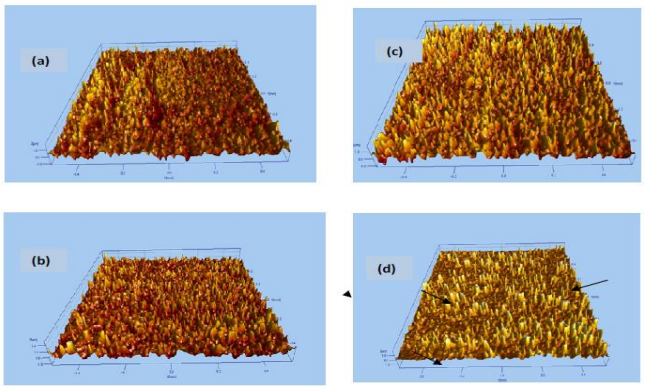

Fig 4: 3-D Optical profiler images obtained of HF etched SS430 for durations (a) 2min (b) 6min (c) 12min (d) 30min. The arrows show over etched patches

The optical profiler has one advantage due to its greater Z-range (typically, 1-2 mm) over an AFM that typically have Z-range upto 7 μm. Though, the optical profiler has a maximum lateral resolution (x-y range) of only approximately 0.6 μm. We have used an optical profiler (NT-3300, Wyko Corp. Tuscon, AZ) for surface roughness measurement of different etched steel surface structures.

The optical profiles of S Steel specimens HF etched for various durations were obtained. The 3D images and profile for the specimen etched for durations of 2, 6, 12, and 30min are shown in Fig. 4.

The progressively increasingly rough textures are visibly apparent for etch time durations from 2min to 12min as in Fig. 4 (a) to Fig. 4 (c). The roughness spikes are clearly visible in the three-dimensional image. The spiked roughness distribution also appears homogeneous as seen from bright and dark contrast in these images. Whereas, for the 30min etch time, there are several locations that appear to be over etched marked by arrows in the Fig. 4(d) where the spikes are non-existent. Several locations were imaged to confirm the above observation.

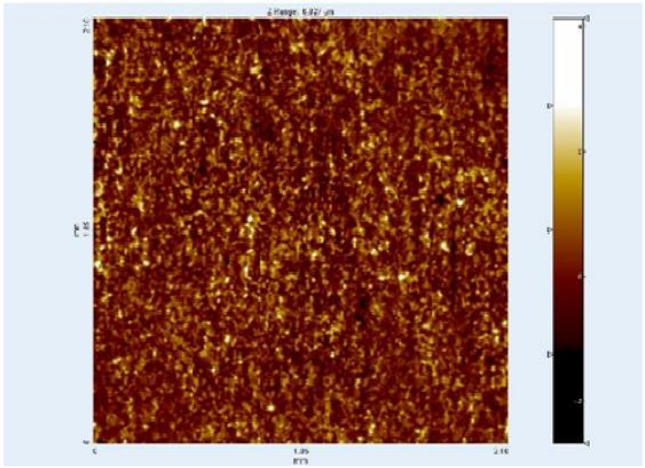

(a)

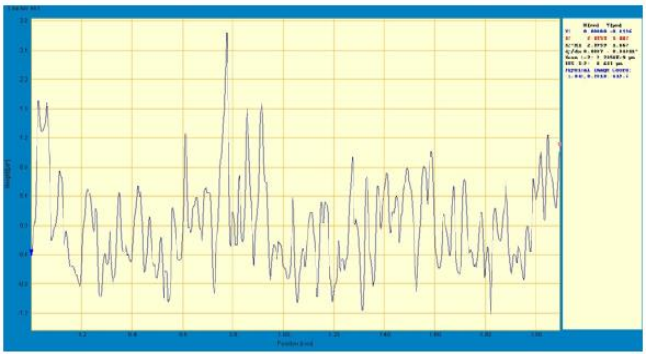

(b)

Fig. 5: (a) Top view of the roughness of HF etched SS430 specimen for duration of 12min imaged by optical surface profiler (b) surface profile at line (2mm) in (a).The peak to valley roughness is approximately 3μm. The RMS roughness 590-725nm

The RMS roughness values of the entire etched specimen were determined by obtaining the line profile as illustrated in Fig. 5 for one of the etched specimens; for the 12min etched SS430 specimen. The line profile shown in Fig 5(b) is taken at the line location shown in top surface image of specimen in Fig 5(a). Line Profiles were obtained at various other locations also to ensure that the line profile data for determining the roughness is as best a representation.

Table II: RMS roughness of various HF etched+HNO3 passivated SS430 specimen

Etch duration	RMS Roughness
2min	100-130nm
6min	140-230nm
12min	590-725nm
20min	610-720nm
30min	590-700nm

From Table II, it may be noticed that the roughness saturates after 12 minutes of etch time as a result the peak to valley roughness values expectedly will be similar for higher etch time. This similarity is clearly seen in line profile in Fig. 6 for the 20min etch specimen, where peak to valley roughness is about the same as in Fig. 6(b) for the 12min etched specimen. The influence of etch time on roughness for various specimen is shown in Fig 7. The roughness increases uniformly from 2 minutes of etch time to 12 minutes and then slowly and marginally increases at 15-20 minutes and slightly reduces for higher etch time of 30 minutes. This behavior shows that a maximum of roughness under the experimented conditions is restricted to about 700nm. The control specimen-as received, degreased and cleaned SS coupons were found to be highly smooth with nano roughness value of <100nm.

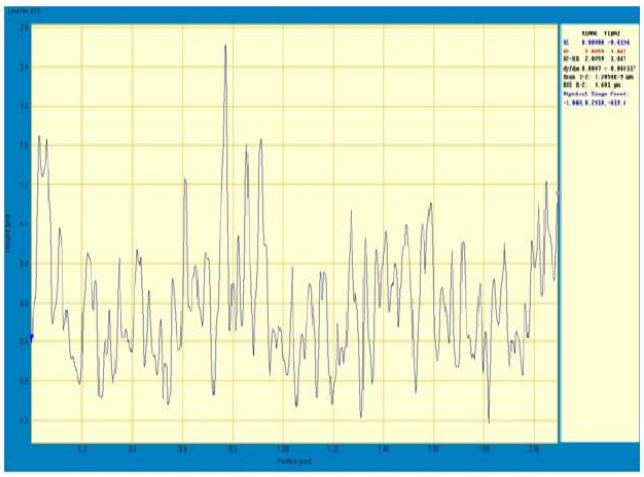

Fig 6: Roughness profile for HF etched specimen for duration of 20minutes; the peak to valley roughness is approximately 3µm, similar to the 12min etched specimen showing a saturation of roughness despite enhanced etching duration.

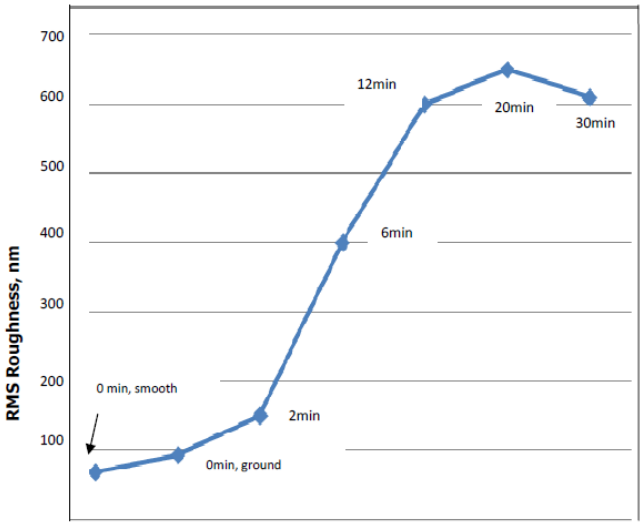

Fig. 7 The RMS roughness of HF etched +HNO3 passivated SS430 specimen

V. CONCLUSION

The basis of the theories on wetting is equilibrium between cohesive and adhesive forces along with surface tension of the liquid drop. Young's theory, Wenzel's model and then CB models are analyzed to conclude that hierarchical structure of nano scale roughness superimposed on primary micro roughness is responsible for the surface to be superhydrophobic. Various processes of creating primary roughness like etching, Laser ablation, sand blasting, deposition method etc. are studied. The methods relevant to this research work are listed and their study related with the current work is made. The prepared roughness samples and nano particles are characterized. The results of their investigation are applied to develop the methodology for creating superhydrophobic surfaces of the stainless steel specimens of a specific composition. These superhydrophobic surface specimens are characterized. The water contact angle measurement of the surfaces is carried out and found to be greater than 150o.

REFERENCES

[1] R.J. Daniello, N.E. Waterhouse, J.P. Rothstein, Drag reduction in turbulent flows over superhydrophobic surfaces, Phys. Fluids. 21 (2009). https://doi.org/ 1I0. 1063/1.3207885.

[2] B.J. Lee, Z. Zhang, S. Baek, S. Kim, D. Kim, K. Yong, Bio-inspired dewetted surfaces based on SiC/Si interlocked structures for enhanced-underwater stability and regenerative-drag reduction capability, Sci. Rep. 6 (2016) 1-l1. https:/ldoi.org/10.1038/srep24653.

[3] F. Van Breugel, M.H. Dickinson, J. Meinwald, Superhydrophobic diving flies (Ephydra hians) and the hypersaline waters of Mono Lake, Proc. Natl. Acad. Sci. U. S. A. 114 (2017) 13483-13488. https:/doi.org/ 10. 1073/pnas. 17 148741|14

[4] F. Lin, L. Shuhong, L. Yingshun, L. Huanjun, Z. Lingjuan, Z. Jin, S. Yanlin, L. Biqian, J. Lei, Z. Daoben, Super-Hydrophobic Surfaces: From Natural to Artificial, Adv. Mater. (2002). https://onlinelibrary. wiley.com/doi/abs/10.1002/adma.200290020.

[5] A.B.D. Cassie, S. Baxter, WETTABILITY OF POROUS SURFACES, Trans. Faraday Soc. 40 (1944).

[6] T. Kamegawa, Y. Shimizu, H. Yamashita, Superhydrophobic surfaces with photocatalytic self cleaning properties by nanocomposite coating of TiO 2 and polytetrafluoroethylene, Adv. Mater. 24 (2012) 3697-3700. https://doi.org/10. 1002/adma.201201037.

[7] S.S. Lathe, P. Sudhagar, A. Devadoss, A.M. Kumar, S. Liu, C. Terashima, K. Nakata, A. Fujishim, Mechanically bendable superhydrophobic steel surface with its self- cleaning and corrosion-resistant properties, J Mater. Chem. A 3 (2015) 10715-10722. https:/doi.org/10. 1039/b000000x.

[8] J.F. Ou, X.Z. Fang, W.J. Zhao, S. Lei, M.S. Xue, F.J. Wang, C.Q. Li, Y.L. Lu, W. Li, Influence of Hydrostatic Pressure on the Corrosion Behavior of Superhydrophobic Surfaces on Bare and Oxidized 5807-5812. Aluminum Substrates, Langmui. 34 (2018) https:/doi.org/ 10.1021/acs.langmuir.8b01 100.

[9] K. Jayaramulu, K.K.R. Datta, C. Rösler, M. Petr, M. Otyepka, R. Zboril, R.A. Fischer, Biomimetic superhydrophobic/superoleophilic highly fluorinated graphene oxide and ZIF-8 composites for oil separation, Angew. Chemie Int. Ed 55 (2016) I178-1182. https://doi.org/10.1002/anie.201507692.

[10] H. Liu, J. Huang, Z. Chen, G. Chen, K.Q. Zhang, S.S. AI-Deyab, Y. Lai, Robust translucent superhydrophobic PDMS/PMMA film by facile one-step spray for self-cleaning and efficient emulsion separation, Chem. Eng. J. 330 (2017) 26-35. https://doi.org/10.1016fj.cej.2017.07.114.

[11] M. Kharati-Koopaee, M.R. Akhtari, Numerical study of fluid flow and heat transfer phenomenon within microchannels comprising different superhydrophobic structures, Int. J. Therm. Sci. 124 (2018) S36-546. https:lldoi.org/ 10. 1016/j.ijthermalsci.2017.11.004.

[12] J.P. Rothstein, Slip on superhydrophobic surfaces, Annu. Rev. Fluid Mech. 42 (2010) 89-109. https://doi.org/ 10.1146/annurev-fluid-121 108-145558.

[13] H. Ling, S. Srinivasan, K. Golovin, G.H. McKinley, A. Tuteja, J. Katz, High-resolution velocity measurement in the inner part of turbulent boundary layers over super-hydrophobic surfaces, J. Fluid Mech. 801 (2016) 670-703. https://doi.org/10.1017jfm.2016.450.

[14] H. Park, C.H. Choi, C.J. Kim, Superhydrophobic drag reduction in turbulent flows: a critical review, Exp. Fluids. 62 (2021) 1-29. https:lldoi.org/ 10.1007/s00348-02 1-03322-4.

[15] C.W. Extrand, Repellency of the Lotus Leaf: Resistance to Water Intrusion under Hydrostatic Pressure, Langmuir. 27 (2011) 6920-6925. https://doi.org/10. 1021/Na201032p.

[16] P. Papadopoulos, L. Mammen, X. Deng, D. Vollmer, H.-J. Butt, How superhydrophobicity breaks down, Proc. Natl. Acad. Sci. I 10 (2013) 3254-3258. https://doi.org/10.1073/pnas. 1218673110.